

Platelets and the $\langle 110 \rangle a_0/4$ $\{001\}$ stacking fault in diamond

J. P. Goss and P. R. Briddon

School of Natural Sciences, University of Newcastle upon Tyne, Newcastle upon Tyne, NE1 7RU, United Kingdom

R. Jones

School of Physics, The University of Exeter, Exeter EX4 4QL, United Kingdom

M. I. Heggie

Department of Chemistry, University of Sussex, Brighton, E Sussex, BN1 9QJ, United Kingdom

(Received 14 December 2005; published 15 March 2006)

Electron microscopy reveals the presence of $\{001\}$ platelets in annealed, nitrogen containing diamond. These extended planar defects give rise to a large displacement of the surrounding material, are correlated with luminescence and optical absorption, and are characterized by the B' vibrational band above the one-phonon maximum. A recent proposal for an atomic structure for these defects is made up from a $\langle 110 \rangle a_0/4$ shear in the $\{001\}$ plane, resulting in C-C double bonds aligned along $\langle 001 \rangle$. We show here that not only is this structure *inconsistent with* experimental observations, but it is unstable and reconstructs to form a largely passive stacking fault defect which also has properties inconsistent with the platelet.

DOI: 10.1103/PhysRevB.73.115204

PACS number(s): 61.72.Ji, 61.72.Bb, 71.20.Mq, 71.23.An

I. INTRODUCTION

Diamond is a material of extremes, with high thermal conductivity, intrinsic carrier mobilities, and hardness. Natural diamond most commonly contains nitrogen as a significant impurity, with material categorized by the dominant form of N-containing defect. In most natural material nitrogen is aggregated, with the most stable form being made up from four nitrogen atoms neighboring a lattice vacancy, termed a B center. The formation of B centers is often accompanied by the formation of large, planar defects called platelets, seen in electron microscopy.

These extended defects lie in $\{001\}$ planes and give rise to a number of properties. Since we extensively reviewed the experiment previously,¹ we simply list some key points here:

1. The displacement of the surrounding lattice due to the presence of the platelets is $0.33\text{--}0.40 a_0$ perpendicular to the plane of the defect, with the larger value corresponding to so-called giant ($1 \mu\text{m}$) platelets.²⁻⁶

2. The platelets are often seen to be rectangular in plan, with *inequivalent* $\langle 110 \rangle$ and $\langle 1\bar{1}0 \rangle$ projections.

3. An infrared absorption band labeled B' with a peak lying between 1358 and 1378 cm^{-1} depending on the size of the platelet⁷ (lower frequencies corresponding to larger platelet) is correlated with the platelet concentration.

4. A broad emission peak is seen centered at 1.25 eV ,^{8,9} with the intensity strongly polarized with the incident electric field within the plane of the defect.¹⁰ Other bands lying at 4.4 and 4.6 eV are seen both in absorption and emission.¹¹ Experiment has not determined whether the optical activity is intrinsic to the platelet or a consequence of defects within or close to them.

5. There is only occasional weak periodicity within the plane, with a period of $\sqrt{8}a_0$ being reported.³

6. There is a direct relationship between the formation of platelets and the nitrogen containing B centers.¹²

The atomic structure and chemical composition of the platelets has been the subject of much debate, and we previously presented the results of calculations on a model based upon self-interstitials¹ first proposed by Humble.¹³ More recently, Miranda *et al.*¹⁴ argued that this model could not be correct based largely on the energetics. Instead they proposed that a structure generated from a $\langle 110 \rangle a_0/4$ shear of the $\{001\}$ plane could more naturally explain the observations. In this structure (shown schematically in Fig. 1) the core of the stacking fault is made up from C-C double bonds similar to those in ethylene.

The suggestion is that, in contrast to the self-interstitial model, this ethylene-bonded stacking fault (EBSF) has gap states which provide the mechanism for the optical emission and absorption. Additionally, this model more obviously gives rise to the nonequivalence of the $\langle 110 \rangle$ and $\langle 1\bar{1}0 \rangle$ directions than the arrangements of blocks of four self-interstitials.¹ They were also able to explain the vibrational properties, but misinterpreted the normal displacement, which we view as a critical failure of their model.^{15,16}

However, we shall show in this paper that the properties of the EBSF not only fail to give rise to the $[001]$ lattice

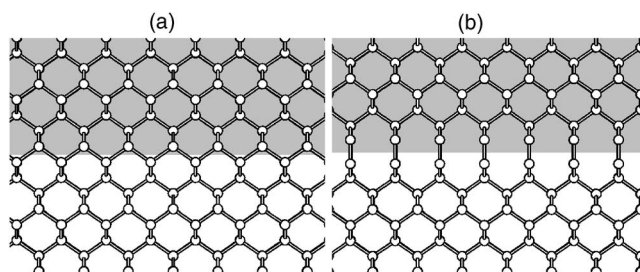


FIG. 1. Diagram of (a) bulk diamond and (b) the $\{001\}$ planar defect created subsequent to a $\langle 110 \rangle a_0/4$ shear projected onto the $(1\bar{1}0)$ plane with $[001]$ vertical. The shaded region indicates the sheared part of the material.

displacement, but cannot easily explain the optical properties, lack of periodicity, or vibrational properties. More significantly, this structure is at best metastable with respect to a simple reconstruction, and would not be stable at the high temperatures at which platelets form.

II. METHOD

Calculations were carried out using the local-spin-density-functional technique implemented in AIMPRO (Ab Initio Modelling Program).¹⁷ Core electrons are eliminated by using norm-conserving pseudo-potentials.¹⁸

The wave function basis consists of atom-centered Gaussians.¹⁹ We use independent s and p Gaussians with four widths, plus one further set of d Gaussians. The charge density is Fourier transformed using plane waves with a cut-off of 300 Ry, yielding total energies converged to ~ 1 meV. The lattice constant and bulk modulus are within ~ 1 and 5%, respectively, of experimental, while the direct and indirect band gaps at 5.68 and 4.26 eV, respectively, are close to previously published plane-wave values.²⁰

The formation energy is calculated using²¹

$$E^f = E - N\mu_C, \quad (1)$$

where E is the calculated total energy, N is the number of atoms in the system, and μ_C is the chemical potential of carbon, taken to be the energy per atom of diamond.

The $\{001\}$ planar stacking fault made up from shearing by $\langle 110 \rangle a_0/4$ may be modeled rather simply in a periodic geometry. One starts with a nonprimitive bulk diamond cell with lattice vectors $\vec{v}_1 = [1 \bar{1} 0]a_0/2$, $\vec{v}_2 = [1 1 0]a_0/2$, and $\vec{v}_3 = [0 0 n_{\text{layer}}]a_0$. This contains $4n_{\text{layer}}$ atoms, each corresponding to a different $\{001\}$ plane. The addition of the shear modifies \vec{v}_3 which is then $[1 1 4n_{\text{layer}}]a_0/4$. A pure shear does not change the volume of the cell, which has a cross-sectional area of $a_0^2/2$.

Although a pure shear does not change the volume of the cell, the presence in a periodic simulation of a planar defect such as a stacking fault in general also results in a dilation or contraction of the lattice perpendicular to the plane of the defect. Changes in the in-plane lattice constants are inhibited by the bulk material either side, and are usually neglected. The total displacement vector due to the presence of the stacking fault is then given by of

$$\vec{d} = [110]a_0/4 + [00\delta]a_0, \quad (2)$$

where we have explicitly resolved in-plane and normal components. The second term is to be compared with the experimental value of $\delta = 0.33\text{--}0.40$.^{2-4,6} To obtain an equilibrium value of δ we have relaxed the sheared structure with a range of n_{layer} and δ .

The Brillouin zone is sampled using the Monkhorst-Pack scheme.²² In the presentation of our results, we refer to the Brillouin-zone sampling using the notation $\text{MP}(n_1, n_2, n_3)$, reflecting a uniform Monkhorst-Pack mesh with n_i points in each reciprocal-lattice direction \vec{b}_i , which in turn may be derived from the direct lattice vectors \vec{v}_i .

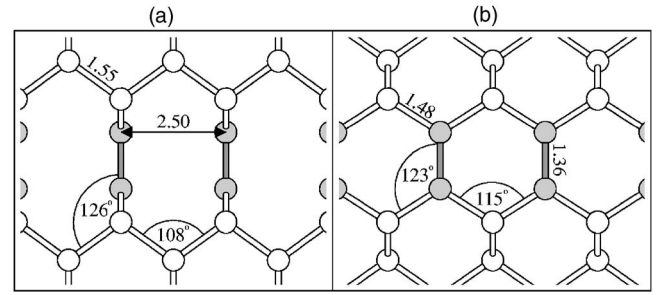


FIG. 2. Detail of the relaxed geometry of the EBSF. Lengths in angstroms. (a) and (b) show projections onto $(1\bar{1}0)$ and (110) planes, respectively, with vertical being $[001]$.

Optical absorption is estimated using the same formalism as that for obtaining electron energy loss spectra,²³ with the absorption coefficient being $4\pi(\text{Im}[\sqrt{\epsilon_1 + i\epsilon_2}])/\lambda$, where ϵ_1 and ϵ_2 are the real and imaginary parts of the dielectric function. This differs from an electronic density of states or examination of a band structure by the inclusion of transition matrix elements. The absorption spectrum is obtained by integrating over the Brillouin zone using Monkhorst-Pack sampling and polynomial broadening of width 0.5 eV. We have not performed any scaling or other operation to correct for the underestimate of the band gap, but instead provide an absorption spectrum for bulk diamond as a comparative reference.

Finally, vibrational modes are calculated by obtaining first-principles force constants, and constructing and diagonalizing the dynamical matrix in the normal way.

III. RESULTS

A. Ethylene structure

We first present the properties calculated for the EBSF of Miranda *et al.*¹⁴ We find a geometry, shown in Fig. 2, very close to theirs. This diagram also shows the nonequivalence of the $\langle 110 \rangle$ and $\langle 1\bar{1}0 \rangle$ projections, as required for a platelet model.

The dependence on the structure and formation energy as a function of the thickness of bulk diamond between stacking faults was obtained for $n_{\text{layer}} = 1$ to 20. For each value of n_{layer} the structures were relaxed with $\delta = 0.0, 0.1, \text{ and } 0.2$ [see Eq. (2)]. A quadratic fit was used to establish the expansion of the lattice required to minimize the total energy. For $n_{\text{layer}} = 10$ we calculated the energy as a function of δ including many more points, as shown in Fig. 3. This yields a minimum in energy very close to that obtained from the quadratic fit, justifying its use elsewhere. For all n_{layer} examined, a value of $\delta = 0.10 \pm 0.01$ was obtained for sampling schemes $\text{MP}(8,8,2)$, $\text{MP}(8,8,4)$, and $\text{MP}(12,12,2)$, and we conclude that this is a converged result. This value of δ falls far short of the experimental values of 0.33–0.40.

The formation energy as a function of n_{layer} rapidly converges to a constant value of 1.7 eV per C-C double bond, provided that the Brillouin zone is sampled sufficiently accurately. We found that $\text{MP}(8,8,2)$, $\text{MP}(8,8,4)$, and $\text{MP}(12,12,2)$ yield formation energies per unit area con-

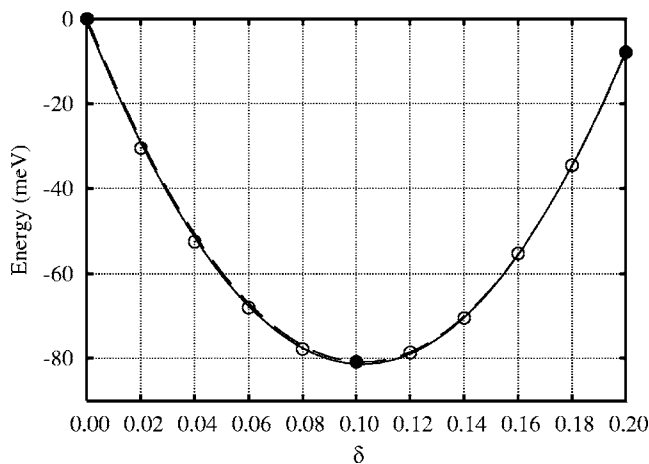


FIG. 3. Formation energy as a function of δ [Eq. (2)] for the defect shown in Fig. 2 with $n_{\text{layer}}=10$. Solid and dashed lines represent a quadratic fit to all and filled points, respectively.

verged to within $\sim 0.2 \text{ J m}^{-2}$, but MP(4,4,2) was insufficient. We find that the EBSF has an energy density of 4.4 J m^{-2} , whereas the self-interstitial model is *much lower* at 2.3 J m^{-2} . An intrinsic stacking fault is calculated to have an energy density of 300 mJ m^{-2} , which compares very favorably with the experimental value²⁴ of $285 \pm 40 \text{ mJ m}^{-2}$, lending support to the other two values. We note that our formation energy for the EBSF exceeds that of 3.42 J m^{-2} from Ref. 14 by about 30%, possibly a consequence of their minimal sampling of the Brillouin zone.

The need for dense in-plane k -point sampling can be understood from a careful examination of the electronic structure. Figure 4 shows the in-plane band structure for the EBSF, revealing a semimetallic nature. The defect bands are already converged for $n_{\text{layer}}=3$, and upon examination of the

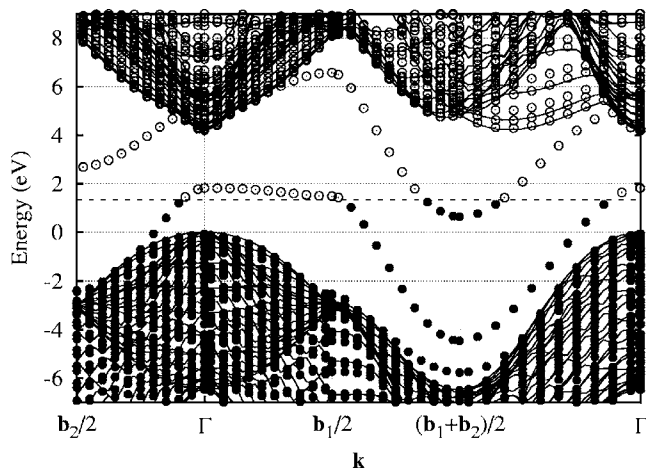


FIG. 4. Band structure of the defect shown in Fig. 2 with $n_{\text{layer}}=10$. Open and closed circles show empty and filled levels, respectively, with the underlying solid lines showing the band structure of bulk diamond. The zero of energy is fixed at the valence band top and the chemical potential of the electrons, as calculated from the self-consistent field, is indicated by the horizontal dashed line. The path taken through the Brillouin zone is given in terms of the reciprocal lattice vectors.

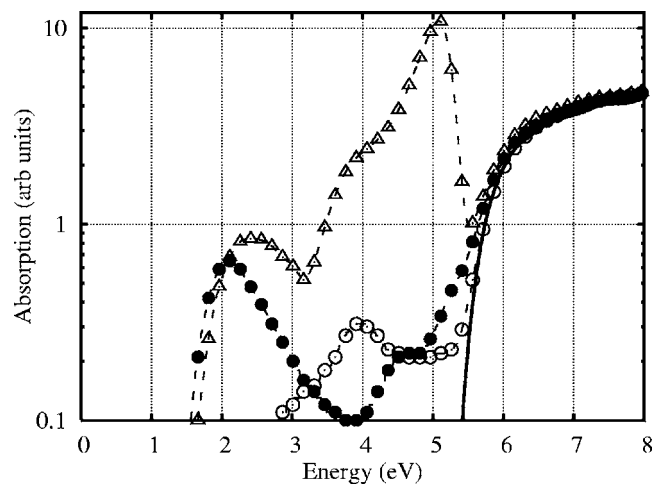


FIG. 5. Optical absorption for the defect shown in Fig. 2 with $n_{\text{layer}}=12$ and MP(30,30,6) sampling. Empty and filled circles show the calculated optical absorption in the $\langle 110 \rangle$, $\langle 1\bar{1}0 \rangle$ polarizations, with the large peak shown in triangles for the polarization approximately along $[001]$. For clarity, only every 15th point calculated is plotted, with the dashed curves showing the full data. The underlying solid line shows the calculation for bulk diamond.

Kohn-Sham orbitals, they can be identified as π and π^* states, as one might expect. The metallic nature would not be resolved within a Γ -point calculation.

Miranda using a single k point determined discrete gap states around -1 , 0 , and 1 eV , and hence argued that the optical spectrum was consistent with the transitions seen experimentally and attributed to the platelet.

However, we find using a converged net of k points that the electronic structure is semimetallic with pockets of electrons and holes (Fig. 4). The calculated absorption spectrum shown in Fig. 5 for vertical transitions only shows a threshold at 2 eV . However, the semimetallic nature of the electronic structure suggests that photoexcited electrons would rapidly thermalize nonradiatively and the luminescence could not then be explained.

Finally, we have calculated the vibrational modes of the EBSF. We do not reproduce the bands at 1373 , 1441 , and 1854 cm^{-1} reported by Miranda *et al.* Instead we find two bands above the one-phonon maximum, which can be characterized as a C-C $[001]$ -stretch mode centered around 1600 cm^{-1} and a torsional mode, as shown schematically in Fig. 6, lying at around 1400 cm^{-1} . These frequencies are consistent with those of graphite. Neither of our modes localized within the stacking fault are infrared active as they are even under inversional symmetry. We find that the vibrational properties of the EBSF are therefore unable to explain the B' band. The difference in our results with those of Miranda *et al.* may be due to the metallic nature in our calculations which would tend to weaken the π bonds via the population of the π^* states.

In summary, in contrast to the claims of Miranda *et al.*,¹⁴ we find that the EBSF cannot easily explain the measured displacement or optical properties of the platelets in diamond. In addition, it is not obvious how one would obtain the observed $\sqrt{8}a_0$ periodicity³ from the stacking fault which

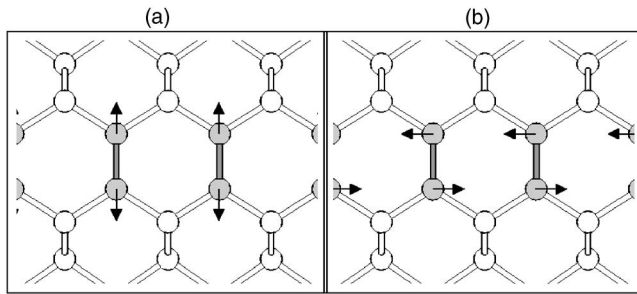


FIG. 6. Schematic of localized vibrational modes for the EBSF, Fig. 2(b). (a) and (b) give rise to bands centered at 1600 and 1400 cm^{-1} , respectively.

actually has a periodicity of $\sqrt{2}a_0/2$, four times smaller than the experimental observation. Neither is it obvious why the periodicity would be weak.

B. (2×1) reconstructions

Notwithstanding the failure of the EBSF model to satisfactorily explain any of the properties of the $\{001\}$ platelets other than the nonequivalence of the $\langle 110 \rangle$ and $\langle 1\bar{1}0 \rangle$ projections, there is a more fundamental reason to reject this structure: It is energetically unstable.

The π orbitals on neighboring ethylene groups point toward one another, and might be expected to reconstruct in line with known systems in diamond such as the R1 paramagnetic center made up from a pair of self-interstitials.^{25,26} Such a reconstruction involves a larger unit cell in the $\{001\}$ plane, which may be why Miranda *et al.* missed these significantly more stable structures.

Figure 7 shows two possible configurations after reconstruction, both of which result in all atoms being fourfold coordinated. Both structures have a lower formation energy than the EBSF, with Fig. 7(b) being the lowest energy structure we have obtained, and can be viewed as resembling two dimerized $\{001\}$ surfaces joined together. The reconstructed planar defect has a formation energy of 2.3 J m^{-2} , which is around the same as the self-interstitial model for the platelet¹ and half that of the EBSF.

The reconstructed bonds are 1.74 and 1.61 \AA for structures (b) and (c), respectively, suggesting that the reconstruction is more effective in the latter case. However, generally formation of five and seven member rings [Fig. 7(b)] is favored over the formation of four and eight member rings [Fig. 7(c)].

In order to assess this new structure in the context of the observed properties of the platelets, we have calculated the displacement normal to the plane of the stacking fault δ , which minimizes the formation energy. We find that it is not significantly different from that of the EBSF and therefore much less than the experimental value.

The band structure is given in Fig. 8. There is only a single empty band close to the conduction band in the otherwise empty band gap. This band is made up from antibonding combinations of sp^3 hybrids, presumably pushed into the band gap by the residual strains. The empty band gap renders

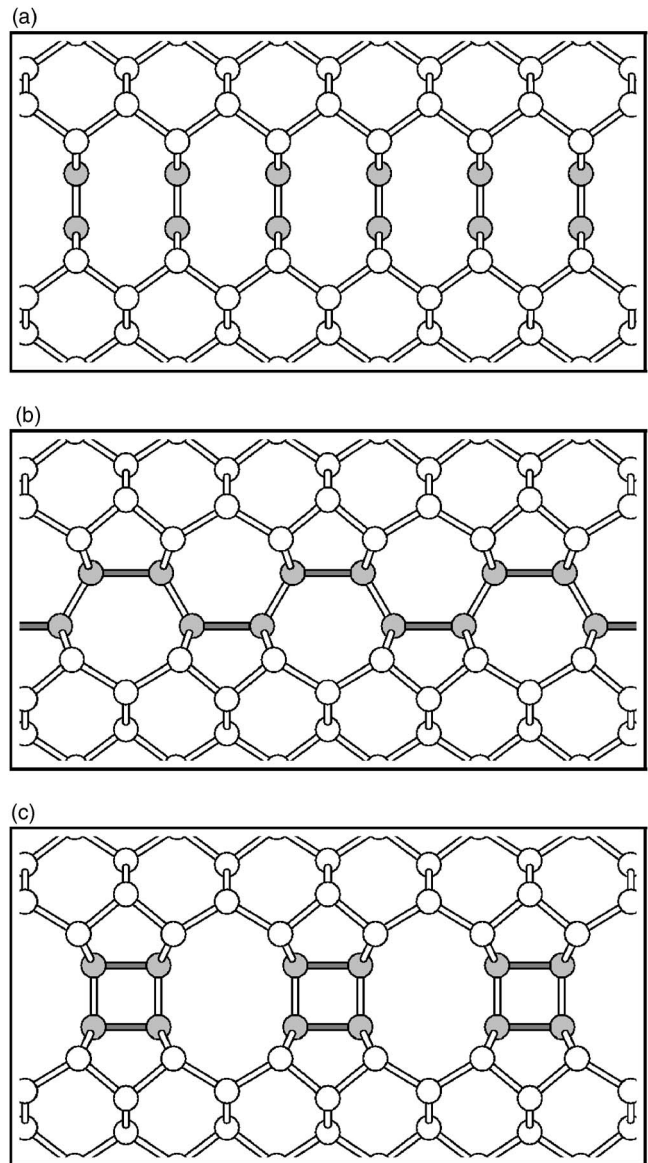


FIG. 7. Schematic diagram showing projections onto the $(1\bar{1}0)$ plane of energetically favorable reconstructions of the EBSF of Miranda *et al.* (Ref. 14). The gray circles show the double layer of atoms constituting the stacking-fault, with gray bonds indicating reconstructions. Vertical is $[001]$. The formation energies of (a), (b), and (c) are 4.4, 2.3 and 3.6 J m^{-2} .

this defect optically inactive in the low energy region associated with the platelets. The optical absorption calculated for the reconstructed stacking fault suggests a shoulder at high energy.

The vibrational modes of the reconstructed stacking fault include a mode around the top of the one-phonon density of states localized in the plane of the defect. The displacements of the atoms in the vibration are shown in Fig. 9. However, the vibration is *infrared inactive* and therefore cannot be correlated with the B' band of the platelets. Other modes with large amplitudes on the stacking fault are resonant with the one-phonon processes of bulk diamond, at variance with B' IR band.

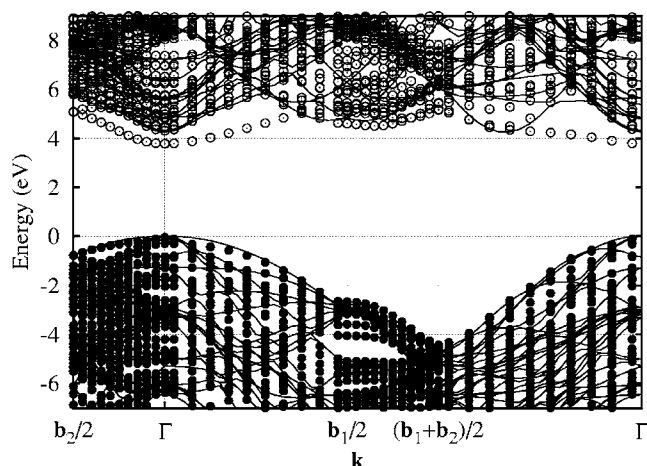


FIG. 8. Band structure of the defect shown in Fig. 7(b) with $n_{\text{layer}}=5$. Open and closed circles show empty and filled levels, respectively, with the underlying solid lines showing the band structure of bulk diamond.

Finally, since it is possible that there is a considerable barrier to obtain the reconstruction from the EBSF, we have examined the barrier explicitly by use of a climbing nudged-elastic-band method.^{27,28} We find no significant barrier exists, suggesting that the C-C double bonds would not form subsequent to the shear, and would certainly be unstable at the very high temperatures associated with the formation of platelets.

IV. SUMMARY

We have presented the structural, electronic, optical, and vibrational properties of ethylene-bonded and reconstructed stacking faults following a $\langle 110 \rangle a_0/4$ shear in the $\{001\}$ plane. At variance with previous reports,¹⁴ from a more detailed analysis of the electronic properties of the EBSF we have shown that the lattice displacement, optical absorption and emission, vibrational properties, and periodicity are at odds with experimental observations for platelets.

More significantly, we have also shown that the EBSF is unstable. It would reconstruct to form a fully fourfold coordinated defect with no gap-states or vibrational modes, and a displacement normal to the plane of the stacking fault that is far smaller than that of the $\{001\}$ platelets. Since this recon-

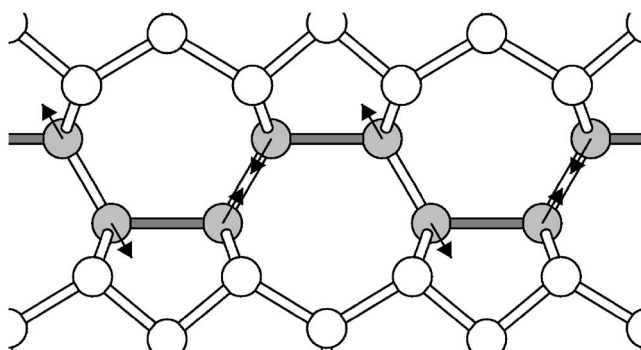


FIG. 9. Schematic of the displacements associated with highest frequency mode confined to the stacking fault shown in Fig. 7(b).

structed form is *significantly* lower in energy, and since we find no barrier to reconstruction, we conclude that an EBSF cannot be responsible for the platelets in diamond. In addition, the reconstructed form also fails to explain the lattice displacement and vibrational properties of platelets and can also be rejected as a model.

In contrast, our previous calculations showed that an array of self-interstitials in a $\{001\}$ plane, *which is much more stable than the EBSF*, explains the displacement and B' vibrational band.¹ Although within the self-interstitial model the optical properties can be understood only by including additional disorder, this is entirely consistent with current experimental data. Indeed, although, as pointed out by Miranda *et al.*, the energetics of formation are relatively high for the self-interstitial model, the formation of platelets occurs in nature over prolonged periods at high temperatures. It is known from experiment that the onset of aggregation of nitrogen into substitutional pairs has substantial barrier at around 5 eV,²⁹ and the formation of B centers one higher still. It is therefore a *requirement* for any model for the formation of platelets to involve a substantial barrier. Finally, the role of B centers in the formation¹² is more direct for a model involving self-interstitials and lattice vacancies than for one involving a shear.

ACKNOWLEDGMENT

We gratefully acknowledge funding provided by EPSRC, UK.

¹J. P. Goss, B. J. Coomer, R. Jones, C. J. Fall, P. R. Briddon, and S. Öberg, Phys. Rev. B **67**, 165208 (2003).

²F. C. Frank, Proc. R. Soc. London, Ser. A **237**, 168 (1956).

³J. C. Barry, L. A. Bursill, and J. L. Hutchison, Philos. Mag. A **51**, 15 (1985).

⁴P. Humble, J. K. MacKenzie, and A. Olsen, Philos. Mag. A **52**, 605 (1985).

⁵P. B. Hirsch, P. Pirouz, and J. C. Barry, Proc. R. Soc. London, Ser. A **407**, 239 (1986).

⁶D. Cherns, K. Kaneko, A. Hovsepien, and A. Lang, Philos. Mag.

A **75**, 1553 (1997).

⁷S. G. Clackson, M. Moore, J. C. Walmsley, and G. S. Woods, Philos. Mag. B **62**, 115 (1990).

⁸D. R. Wright, P. J. Dean, E. C. Lightowers, and C. D. Mobsby, J. Lumin. **4**, 169 (1971).

⁹S. Desgreniers, Y. K. Vohra, and A. L. Ruoff, Solid State Commun. **70**, 705 (1989).

¹⁰I. Kiflawi and A. R. Lang, Nature (London) **267**, 36 (1977).

¹¹E. V. Sobolev, V. E. Il'in, S. V. Lenskaya, and O. P. Yur'eva, J. Appl. Spectrosc. **9**, 1108 (1968).

- ¹²G. S. Woods, Proc. R. Soc. London, Ser. A **407**, 219 (1986).
- ¹³P. Humble, Proc. R. Soc. London, Ser. A **381**, 65 (1982).
- ¹⁴C. R. Miranda, A. Antonelli, and R. W. Nunes, Phys. Rev. Lett. **93**, 265502 (2004).
- ¹⁵R. Jones, M. I. Heggie, and J. P. Goss, Phys. Rev. Lett. **95**, 139601 (2005).
- ¹⁶C. R. Miranda, A. Antonelli, and R. W. Nunes, Phys. Rev. Lett. **95**, 139602 (2005).
- ¹⁷R. Jones and P. R. Briddon, in *Identification of Defects in Semiconductors*, edited by M. Stavola, Semi-conductors and Semimetals Vol. 51A (Academic Press, Boston, 1998), Chap. 6.
- ¹⁸C. Hartwigsen, S. Goedecker, and J. Hutter, Phys. Rev. B **58**, 3641 (1998).
- ¹⁹J. P. Goss, M. J. Shaw, and P. R. Briddon, Top. Appl. Phys. (to be published).
- ²⁰D. A. Liberman, Phys. Rev. B **62**, 6851 (2000).
- ²¹S. B. Zhang and J. E. Northrup, Phys. Rev. Lett. **67**, 2339 (1991).
- ²²H. J. Monkhorst and J. D. Pack, Phys. Rev. B **13**, 5188 (1976).
- ²³C. J. Fall, R. Jones, P. R. Briddon, A. T. Blumenau, T. Frauenheim, and M. I. Heggie, Phys. Rev. B **65**, 245304 (2002).
- ²⁴S. Takeuchi and K. Suzuki, Phys. Status Solidi A **171**, 99 (1999).
- ²⁵D. J. Twitchen, M. E. Newton, J. M. Baker, O. D. Tucker, T. R. Anthony, and W. F. Banholzer, Phys. Rev. B **54**, 6988 (1996).
- ²⁶J. P. Goss, B. J. Coomer, R. Jones, T. D. Shaw, P. R. Briddon, M. Rayson, and S. Öberg, Phys. Rev. B **63**, 195208 (2001).
- ²⁷G. Henkelman, B. P. Uberuaga, and H. Jónsson, J. Chem. Phys. **113**, 9901 (2000).
- ²⁸G. Henkelman and H. Jónsson, J. Chem. Phys. **113**, 9978 (2000).
- ²⁹T. Evans and Z. Qi, Proc. R. Soc. London, Ser. A **381**, 159 (1982).